Understanding the Ring Current Effects on Magnetic Shielding of Hydrogen and Carbon Nuclei in Naphthalene and Anthracene

INMACULADA GARCÍA CUESTA,[1] ALFREDO SÁNCHEZ DE MERÁS,[1] STEFANO PELLONI,[2] PAOLO LAZZERETTI[2]
[1]*Institut de Ciència Molecular, Universitat de València, P.O. Box 22085, E-46071 València, Spain*
[2]*Dipartimento di Chimica dell'Università degli Studi di Modena e Reggio Emilia, Via Campi 183, 41100 Modena, Italy*

Received 7 May 2008; Revised 25 June 2008; Accepted 20 October 1996
DOI 10.1002/jcc.21083
Published online 18 August 2008 in Wiley InterScience (www.interscience.wiley.com).

Abstract: The local response to an external magnetic field normal to the molecular plane of naphthalene and anthracene was investigated via current density and magnetic shielding density maps. The Biot-Savart law shows that the deshielding caused by π-ring currents in naphthalene is stronger for α- than for β-protons due to geometrical factors. The shielding tensor of the carbon nuclei in both molecules is strongly anisotropic and its out-of-plane component determines the up-field chemical shift of ^{13}C in nuclear magnetic resonance spectra. The π-ring currents flowing beyond the C-skeleton in front of a probe carbon nucleus, and on remote parts of the molecular perimeter, yield positive contributions to the out-of-plane component of carbon shielding as big as ≈10–15% of the total values. Near Hartree-Fock estimates of magnetizability and magnetic shielding at the nuclei fully consistent with the current model are reported.

 J Comput Chem 30: 551–564, 2009

Key words: naphthalene; ring currents; proton and carbon chemical shift; current density maps

Introduction

Theoretical studies of the naphthalene and anthracene molecule available so far provide ring current models for magnetic response,[1–3] and predictions of average magnetizability and ^{1}H and ^{13}C magnetic shieldings in reasonable agreement with experimental data from nuclear magnetic resonance (NMR) spectroscopy.[2,3] However, previous theoretical investigations are far from being satisfactory, due to insufficient flexibility of the basis sets adopted, 6-31G** in ref. 1 and (9sp2d/5s2p)→[5s4p1d/3s1p] in refs. 2, 3 Moreover, they do not explain a number of peculiar features that await rationalization from a long time, e.g., (i) the chemical shift between α and β protons, (ii) the different magnitude and the strong upfield chemical shift of nonequivalent carbon nuclei, (iii) the enhanced anisotropy of the ^{13}C shielding tensors, (iv) the contribution of the π-ring currents to the magnetic shielding of hydrogen and carbon nuclei.

Near Hartree-Fock (HF) results are not available for the magnetic properties of the $C_{10}H_8$ molecule, despite the claim of accuracy for results[2] obtained via approaches allowing for continuous translation of the origin of the current density (CTOCD)[4,5] within the damped paramagnetic-zero (PZ2) variant.[6] The magnetic shieldings of ^{1}H predicted via different computational procedures – which would be exactly the same in the HF limit – agree quite well, see Table 3 of ref. 2. However, discrepancies are evident by inspection of Tables 1 and 2, for magnetizabilities and ^{13}C shielding tensors, among common origin (CO) and a series of CTOCD schemes, diamagnetic-zero (DZ), damped (DZ2) variant,[4,6] and undamped paramagnetic-zero (PZ). A similar state of affairs is found for anthracene. Its magnetic response was incompletely explained in the previous paper,[3] and properties evaluated at DZ2 and PZ2 levels of accuracy are slightly different.

Additional Supporting Information may be found in the online version of this article.

Correspondence to: P. Lazzeretti; e-mail: lazzeret@unimo.it

Contract/grant sponsor: NANOQUANT European network; contract/grant number: MRTN-CT-2003-506842

Contract/grant sponsor: Acción Integrada Hispano-Italiana; contract/grant number: HI2004-0243

Contract/grant sponsor: Spanish FEDER + MEC; contract/grant number: CTQ 2007-67143-C02-01/BQU

Contract/grant sponsor: Generalitat valenciana; contract/grant number: ACOMP07/163 GV/2007/093 GVAINF 2007-051

Contract/grant sponsor: Ajudes Investigació UVEG (2006), Italian MIUR (Ministero dell' Università e della Ricerca Scientifica e Tecnologica), Via PRIN funds

More accurate calculations are timely for reliable estimates of near HF magnetic properties of naphthalene and anthracene. The present article also aims at providing the definitive answer to the points (i)–(iv) expounded above by using graphical tools quite practical for modeling the phenomenology of molecules in a magnetic field.

Current Density and Shielding Density Maps

Two thematic issues[7,8] of *Chemical reviews* were dedicated to the basic topics of "Aromaticity" and "Delocalization-Pi and Sigma". The peculiar magnetic behavior associated with induced ring currents in aromatic compounds is frequently related to the cyclic electron delocalization that characterizes such species. Aromaticity definitions have been proposed in terms of magnetic properties.

The magnetic response of a molecule is determined by the current density $\mathbf{J^B}$ induced in the electron cloud by an external magnetic field $\mathbf{B}$. A ring-current model (RCM) has been developed[7,9,10] to rationalize the mechanisms causing down-field chemical shift of aromatic protons. However, the RCM is not suitable to explain the strong anisotropy of carbon shielding observed in NMR spectra of arenes. Studies of typical aromatic, anti-aromatic, and non aromatic molecules[3,11–19] have analyzed the ring current effects on nuclear magnetic shielding. *Ab initio* maps of magnetic shielding density[20,21] provide detailed information by the differential Biot-Savart (DBS) law of classical electromagnetism.[22]

The history of the magnetic shielding function and related calculations are found in a recent review by Heine, Corminboeuf and Seifert,[23] see also a seminal paper by Johnson and Bovey.[24] The response of a molecule to an applied external magnetic field has been evaluated by graphical representation of the induced magnetic field by Merino et al.[25] and Heine et al.[26]

The DBS based ring-current model[11,13,14,27] gives the element of magnetic field induced by the current density $\mathbf{J^B}(\mathbf{r})$ on a probe nuclear magnetic dipole $\mathbf{m}_I$, at the observation point $\mathbf{R}_I$ where the I-th nucleus is placed,

$$d\mathbf{B}_{ind}(\mathbf{R}_I) = \frac{\mu_0}{4\pi}\mathbf{J^B}(\mathbf{r}) \times \frac{\mathbf{R}_I - \mathbf{r}}{|\mathbf{R}_I - \mathbf{r}|^3} d^3r. \quad (1)$$

By integrating over the spatial coordinates, the integral Biot-Savart (IBS) law

$$B_{ind,\alpha}(\mathbf{R}_I) = -\sigma_{\alpha\beta}(\mathbf{R}_I)B_\beta, \quad (2)$$

which gives the total magnetic field flux density induced at $\mathbf{R}_I$, is obtained. The local shielding at the observation point is defined

$$\sigma_{\alpha\delta}(\mathbf{R}_I) \equiv \sigma^I_{\alpha\delta} = -\frac{\mu_0}{4\pi}\epsilon_{\alpha\beta\gamma}\int \frac{r_\beta - R_{I\beta}}{|\mathbf{r} - \mathbf{R}_I|^3}\mathcal{J}^{B_\delta}_\gamma(\mathbf{r})d^3r, \quad (3)$$

introducing the current density tensor[5]

$$\mathcal{J}^{B_\beta}_\alpha(\mathbf{r}) = \frac{\partial}{\partial B_\beta} J^{\mathbf{B}}_\alpha(\mathbf{r}). \quad (4)$$

The integrand function in the integral Biot-Savart (IBS) law (2)–(3) is a shielding density tensor, with zz component[20,21]

$$\Sigma^I_{zz}(\mathbf{r}) = -\frac{\mu_0}{4\pi}\epsilon_{z\beta\gamma}\frac{r_\beta - R_{I\beta}}{|\mathbf{r} - \mathbf{R}_I|^3}\mathcal{J}^{B_z}_\gamma(\mathbf{r}). \quad (5)$$

Therefore, the element of out-of-plane magnetic field, induced by the current density at point $\mathbf{r}$ on xy planes parallel to that of the molecule (which, in turn, has been generated by the external magnetic field B_z), is rewritten

$$dB_{ind,z}(\mathbf{R}_I) = -\Sigma^I_{zz}(\mathbf{r})B_z d^3r. \quad (6)$$

Assuming that the modulus of the π-ring currents is almost the same all over a given circuit, e.g., the perimeter of an aromatic molecule, shielding or deshielding effects on the probe depend essentially on geometrical factors. In fact, according to eq. (1), the sign of $dB_{ind,z}(\mathbf{R}_I)$, induced on nucleus I by the current density $\mathbf{J^B}(\mathbf{r})$, is determined by the sine of the angle θ (positive for an anticlockwise rotation) between the vectors $\mathbf{J^B}(\mathbf{r})$ and $\mathbf{R}_I - \mathbf{r}$. For $0 < \theta < \pi(\pi < \theta < 2\pi)$, the element of flux density is positive (negative) and reinforces (diminishes) the applied field. Therefore, according to eqs. (2) and (5), the local current density $\mathbf{J^B}(\mathbf{r})$, generated by an external magnetic field B_z perpendicular to the molecular plane of arenes, deshields (shields) the probe by providing a negative (positive) contribution to $\Sigma^I_{zz}(\mathbf{r})$.

Response of Arenes to a Magnetic Field Normal to the Molecular Plane

In the benzene molecule in the presence of a uniform static magnetic field perpendicular to the molecular plane, the π-ring currents reinforce the external magnetic field at the site of a proton and reduce the out-of-plane component σ^H_{zz} of the proton shielding tensor. The deshielding mechanism takes place in a small area nearby a hydrogen nucleus, but weaker shielding contributions are provided by the return electron flow in more distant regions, as shown by shielding density maps.[11–13,27] It has also been demonstrated that, for a given carbon nucleus of benzene, the local π-ring currents have no effect on σ^C_{zz}, whereas, the shielding contribution from the remote carbon atoms is ~10% of the total out-of-plane component.[14,28]

On the other hand, many aspects have not yet been explained and a refined model is not available for interpreting the magnetic response of systems that contain two fused aromatic cycles, like naphthalene[1,2] and aza-naphthalenes.[29] Current density maps have been reported for anthracene at CTOCD-DZ[1] and CTOCD-DZ2[3] coupled Hartree-Fock (CHF) level. Polycyclic aromatic hydrocarbons (PAH) sustain π-ring currents over the molecular perimeter as the mono-cyclic systems, but also display typical features, e.g., weak diamagnetic π-vortices about the center of each ring and the midpoint of the C–C bond connecting them,[2,29] see Figures 1 and 4 in this work.

Fused hetero-bicycles,[15–17,19] were shown to have properties typical of aromatic molecules. In particular, the tetra-azanaphthalenes with a pair of nitrogen atoms in each ring are diatropic systems, whose magnetic response to a magnetic field perpendicular to the molecular plane resembles naphthalene.[29] Current

density maps show that the intensity of the π-electron currents over the molecular skeleton is approximately uniform with slightly higher intensity in the proximity of the peripheral carbon and nitrogen atoms, which is consistent with the RCM.

In the present study, the CTOCD-DZ2 procedure[4–6] implemented in the SYSMO code[30] was used at the CHF level employing a non contracted (13s10p5d2f/8s4p1d) basis set.[12] For the sake of consistency, the molecular geometries of naphthalene and anthracene have been optimized at the self-consistent-field level via the GAUSSIAN code[31] using the same basis set. The excellent quality of the present CHF calculation, the most accurate reported so far for magnetic properties of naphthalene and anthracene, was assessed by a series of auxiliary tools, c.f., the Supplementary Material Available (SMA) for extended documentation.

Theoretical magnetizabilities and nuclear magnetic shieldings of naphthalene and anthracene from all CTOCD schemes are origin independent. Near CHF estimates for magnetizability of naphthalene evaluated in this study, (in $JT^{-2} \times 10^{-29}$ per molecule) are $\chi_{xx} = -97.1$, $\chi_{yy} = -89.6$, $\chi_{zz} = -310.7$, $\chi_{av} = -165.8$. The experimental χ_{av} values[32] are in the range -150.7 to -154.3. Near CHF estimates for magnetizability of anthracene, in the same units, are $\chi_{xx} = -132.8$, $\chi_{yy} = -116.4$, $\chi_{zz} = -442.7$, $\chi_{av} = -230.6$. The experimental χ_{av} values[32] are in the range -215.3 to -222.8 $JT^{-2} \times 10^{-29}$ per molecule. The magnetic anisotropy of these compounds is strong, as expected for diatropic molecules whose π electrons sustain intense ring currents.

One can observe that the CHF approach overemphasizes diamagnetism of naphthalene and anthracene. Further investigations

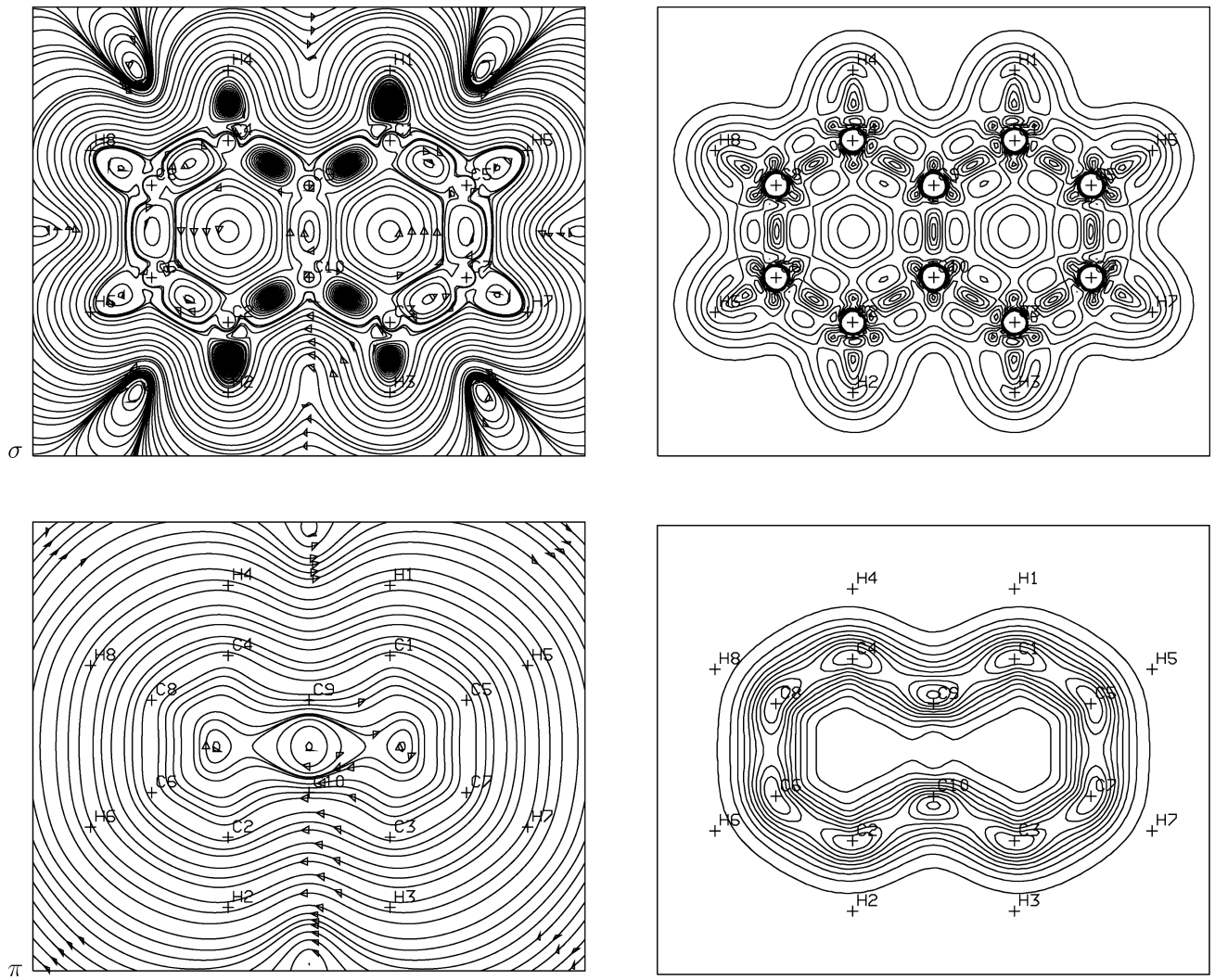

Figure 1. Streamlines and contour levels for the modulus of the total current density on the molecular plane of naphthalene (above) and π-electron contributions on a plane at 0.75 bohr (below). Nuclear positions are marked with crosses. The applied magnetic field (of unit magnitude) points outward and diamagnetic flow is clockwise. The maximum modulus (contour step) values are 1.97 (cut to 0.2), and 0.09 (0.02 and 0.009), respectively, in au.

Table 1. Nuclear magnetic shieldings of symmetry unique atoms in naphthalene molecule (in ppm).[a]

Atom	Contr.	*xy*	*yx*	*xx*	*yy*	*zz*	*av*
C_1	σ + core					156.56	
	π					15.82	
	Total	−21.21	−27.08	49.64	−54.69	172.38	55.78
	EXP[b,c]			46 (41)	−60 (−59)	171 (174)[d]	58.0,57.7[e]
C_5	σ + core					167.15	
	π					18.14	
	Total	−57.50	−55.05	−15.66	5.64	185.28	58.42
	EXP[b,c]			−28 (−29)	12	183 (184)[d]	60.1,59.7[e]
C_9	σ + core					175.90	
	π					26.24	
	Total	0.00	0.00	−37.10	−21.74	202.14	47.77
	EXP[b,c]			−39	−20	200[d]	52.4,52.07[e]
H_1	σ + core					23.11	
	π					−4.65	
	Total	−0.86	−0.74	28.97	23.88	18.46	23.77
	EXP[f]						23.02
H_5	σ + core					23.19	
	π					−3.52	
	Total	−1.82	−1.46	26.40	26.77	19.67	24.28
	EXP[f]						23.37

[a] Via the CTOCD-DZ2 approach.

[b] The individual components of the chemical shift tensor δ_{ii} (no sum over repeated Latin indices) obtained experimentally are related to the absolute shielding tensor components σ_{ii} by the equation[36] $\delta_{ii} = (\sigma_{REF} - \sigma_{ii})/(1 - \sigma_{REF}) \approx \sigma_{REF} - \sigma_{ii}$. The relation used to estimate the experimental shielding components $\sigma_{ii,N}$, $i = x, y, z$ of a carbon nucleus in naphthalene is $\sigma_{ii,N} = \sigma_{ii,B} + \delta_{ii,B} - \delta_{ii,N}$; near Hartree-Fock values of the absolute shielding in benzene are[14] $\sigma_{xx,B} = -72.0$, $\sigma_{yy,B} = 43.0$, and $\sigma_{zz,B} = 185.0$ ppm for C1, $\sigma_{xx,B} = 14.1$, $\sigma_{yy,B} = -43.0$, and $\sigma_{zz,B} = 185.0$ ppm for C2; corresponding chemical shift tensor components are[37] $\delta_{xx,B} = 234$, $\delta_{yy,B} = 146$ for C1, $\delta_{xx,B} = 168$, $\delta_{yy,B} = 212$ ppm for C2, via Euler rotations $\alpha = 0$, $\beta = 0$, $\gamma = \pi/3$ (the x and y axes for benzene should be interchanged for referencing naphthalene data). The $\delta_{ii,N}$ experimental values are from Table 1 of ref. 38, see also ref. 39, 40. The entries in brackets are relative to a symmetry related C nucleus, see Table 1 and Fig. 2 of ref. 38.

[c] The relation used to estimate the average shielding $\sigma_{av,N}$ of a carbon nucleus in naphthalene is $\sigma_{av,N} = \sigma_{av,B} + \delta_B - \delta_N$, where $\sigma_{av,B} = 57.2$ ppm is the absolute average shielding in benzene,[41] the chemical shift of benzene is $\delta_B = 128.5$ ppm,[35,42] and the chemical shifts δ_N in naphthalene are 127.7[42] and 128.0[35] for C1, 125.6[42] and 126.0[35] for C5, 133.3[42] and 133.7[35] for C9.

[d] The $\delta_{33,N}$ experimental values[38] are 22.8 (20.4) for C1, 11.1 (10.4) for C2, and −5.9 for C9. Overall errors due to referencing and fitting approach ±3 ppm for benzene,[37] the standard deviation of the fit to the naphthalene data is 0.378 ppm.[38]

[e] The estimated average shieldings do not coincide with $(\sigma_{xx} + \sigma_{yy} + \sigma_{zz})/3$ from columns 4–6 of the table. These values were obtained from different sources[35,42] via different criteria, see footnote.[c]

[f] Quoted in ref. 2

are needed to evaluate electron correlation effects and other contributions possibly arising from molecular vibration.

Near CHF estimates of the out-of-plane component of nuclear magnetic shielding tensors (i.e., the quantity biased by ring currents), partitioned into σ+core- and π-electron orbital contributions, are reported in Tables 1 and 2.

The magnetic properties determined at the CTOCD-DZ-RHF/6-31G** level of theory[1*] are unreliable: values predicted for nuclear shieldings are wrong in sign and magnitude, as shown in earlier papers.[4,33] CTOCD-DZ is usually unsuitable to obtain accurate

[*] The CTOCD-DZ tensor components of carbon shielding calculated via the 6-31G** basis set in ref. 1 (not reported by the authors) are very poor. For naphthalene: $\sigma_{xx}^{C1} \approx -127$, $\sigma_{yy}^{C1} \approx -215$, $\sigma_{zz}^{C1} \approx 3$, $\sigma_{xx}^{C5} \approx -181$, $\sigma_{yy}^{C5} \approx -167$, $\sigma_{zz}^{C5} \approx 16$, $\sigma_{xx}^{C9} \approx -196$, $\sigma_{yy}^{C9} \approx -183$, $\sigma_{zz}^{C9} \approx 26$, in ppm. The carbon shielding is wrong in sign and magnitude, compare with the values reported in Table 1 of the present study. The CTOCD-DZ 6-31G** results for hydrogen shielding in naphthalene are also inaccurate: $\sigma_{xx}^{H1} \approx 26$, $\sigma_{yy}^{H1} \approx 18$, $\sigma_{zz}^{H1} \approx 17$, $\sigma_{xx}^{H5} \approx 19$, $\sigma_{yy}^{H5} \approx 23$, $\sigma_{zz}^{H5} \approx 18$, see Table 1. The CTOCD-DZ/6-31G** components of the magnetizability tensor (in $JT^{-2} \times 10^{-29}$ per molecule) $\chi_{xx} = -35.0$, $\chi_{yy} = -35.5$, $\chi_{zz} = -291.8$, and the average value $\chi_{av} = -120.8$ are far from the near Hartree-Fock values calculated in the present study, $\chi_{xx} = -97.1$, $\chi_{yy} = -89.6$, $\chi_{zz} = -310.7$, and $\chi_{av} = -165.8$. A similar failure was found for anthracene. Therefore the qualitative CTOCD-DZ/6-31G** current models proposed for naphthalene and anthracene in ref. 1 are unacceptable for rationalization of magnetic properties. Remarkably enough, almost correct predictions of carbon shielding (and more reliable models for the current density in the vicinity of the nuclei) would have been obtained via the modest 6-31 G** basis allowing for the damped CTOCD-DZ2 procedure.

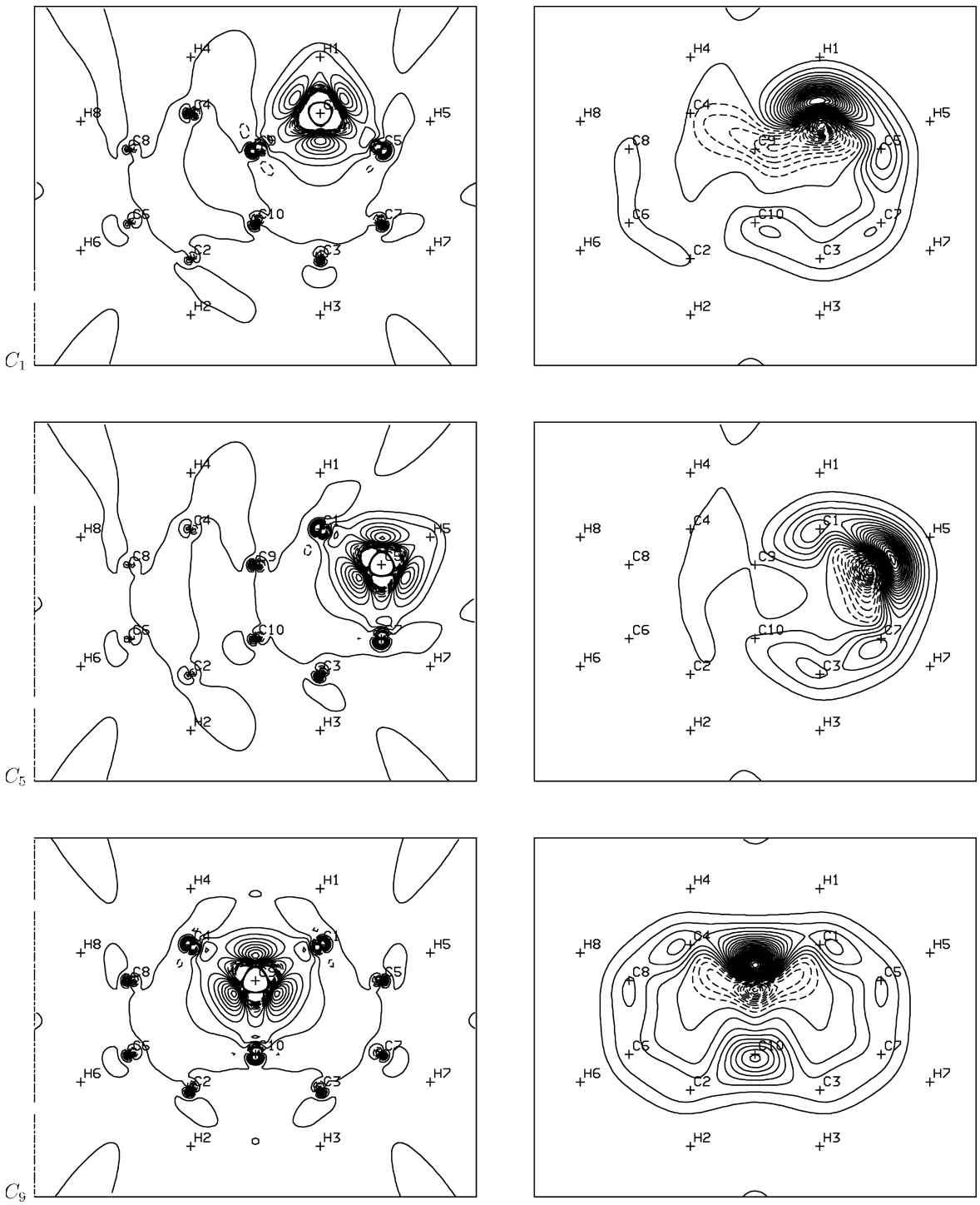

Figure 2. From top to bottom, magnetic shielding densities Σ_{zz}^{C1}, Σ_{zz}^{C5}, and Σ_{zz}^{C9} in naphthalene. σ-electron (π-electron) contributions on the molecular plane (on a plane at 0.75 bohr) are given on the left (right). In the contour map solid (dashed) lines mean positive (negative) values. Minimum (maximum) value of σ contributions are cut to -0.1 (0.1) and the contour step is 0.01. Minimum (maximum) values of π-contributions are -0.019 (0.021), -0.019 (0.021), and -0.011 (0.029) for C1, C5, and C9, respectively. The contour step is 0.001.

maps of $\mathbf{J}^{\mathbf{B}}(\mathbf{r})$, unless extended basis sets are employed. Description lacks precision in the vicinity of the nuclei.[34] In these regions use of the damped DZ2 or PZ2 procedures[6] is recommended for 6-31G** basis set calculations.

An external magnetic field **B** perpendicular to the σ_h plane of arenes induces electronic flow, represented in Figures 1 and 4 by maps of σ-electron current density on this plane, and of π-ring currents on a plane at 0.75 bohr above, i.e., in a domain characterized by nearly maximum π-electron density for these systems. As the molecular plane is a nodal region for the π-electrons, the σ-electron contributions coincide with the total flow on the σ_h plane.

The σ-current density field of naphthalene, see Figure 1, presents distinctive features, a diamagnetic (clockwise) main stream in the molecular periphery, and two paramagnetic vortices about the ring centers,[2,10] as confirmed by the present more accurate study. Local diamagnetic vortices and spiral flows (in the vicinity of foci at which the current has a perpendicular component) are visible in the region of peripheral C–C bonds. The intensity of the diatropic π-electron current is virtually the same all over the carbon skeleton ($\approx$0.06 au) with a small enhancement in the proximity the nuclei ($\approx$0.08) – slightly higher about the bridge carbon nuclei C9 and C10 ($\approx$0.09 au).

The calculated average in-plane $\sigma_{\perp}^{H} \equiv (\sigma_{xx}^{H} + \sigma_{yy}^{H})/2$ components of nonequivalent protons are nearly the same, 26.43 and 26.59 ppm respectively for H1(α) and H5(β). Therefore, the difference of chemical shift observed in NMR spectra in isotropic phase, 0.35 ppm[35] (c.f. the shift $\sigma^{H5} - \sigma^{H1} \approx 0.51$ ppm calculated in this work), depends mainly on different values of σ_{zz}^{H} for the two sites. On the

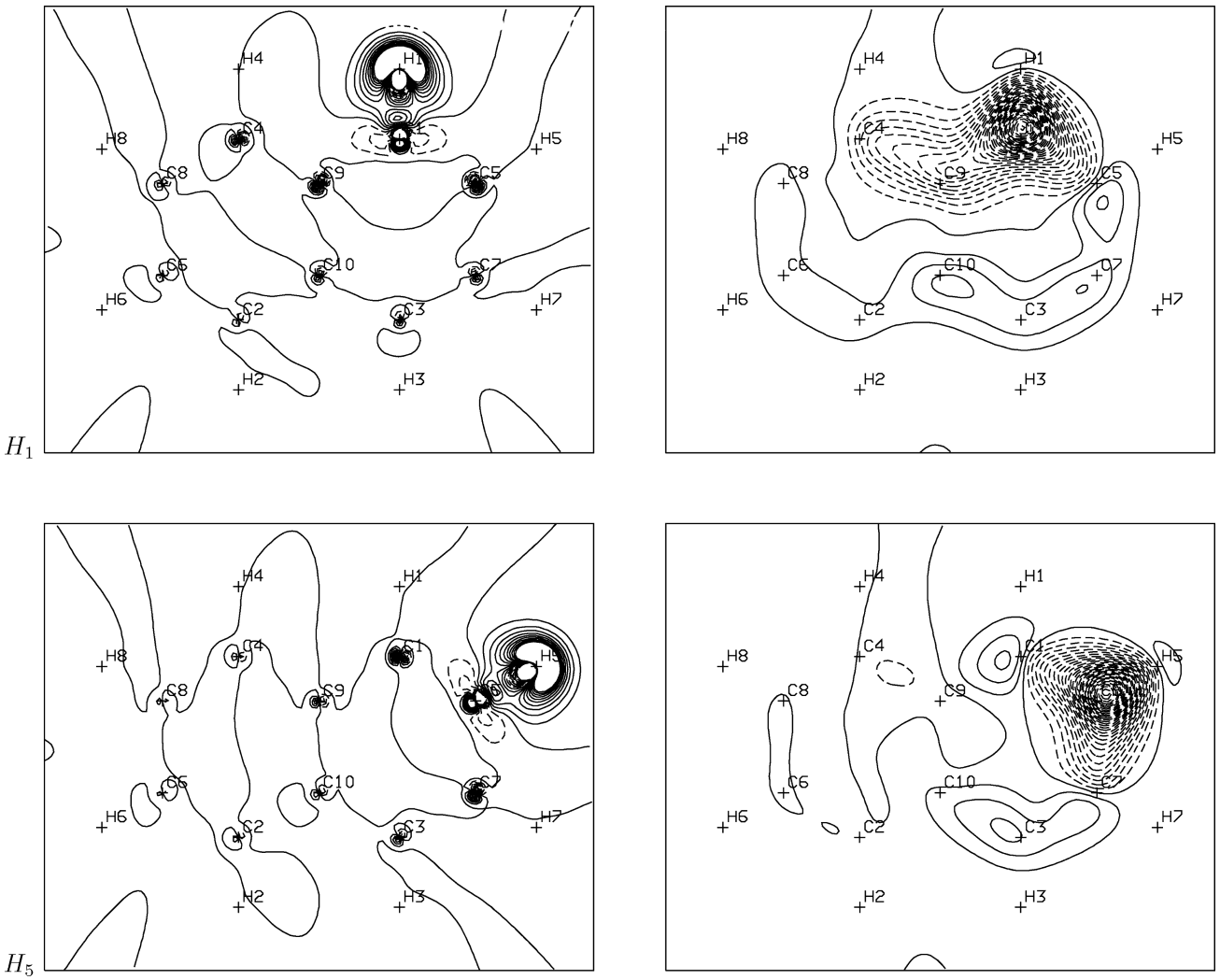

Figure 3. Magnetic shielding densities Σ_{zz}^{H1} (above) and Σ_{zz}^{H5} (below) in naphthalene. σ-electron (π-electron) contributions on the molecular plane (on a plane at 0.75 bohr) are given on the left (right). Plotting conventions are the same as in Figure 2. Minimum (maximum) values of σ-electron contributions, in au, are cut to -0.1 (0.1 for all protons and the contour step is 0.01. Minimum (maximum) values of π-electron contributions, in au, are -0.015 (0.0017) and -0.015 (0.0016) for H1 and H5, respectively. The contour step is 0.0005.

other hand, the σ-currents provide shielding contributions of almost the same magnitude to the out-of-plane component σ_{zz}^H of proton shielding, as can be observed by the values 23.11 and 23.19 ppm in Table 1 (c.f. the value 23.34 ppm in benzene[12]). However, the deshielding operated by the π-ring currents is quite different, c.f., the negative contributions -4.65 and -3.52 ppm to σ_{zz}^H. Therefore, the shift between α and β protons of naphthalene is essentially due to π-ring currents that bias the out-of-plane component σ_{zz}^H to different extent.

The DBS law yields a simple explanation of this phenomenology. Maps are reported for the total shielding density[20,21] $\Sigma_{zz}^C(\mathbf{r})$ on the molecular plane in Figure 2. Analogous maps of $\Sigma_{zz}^I(\mathbf{r})$ shielding density, showing contributions from the π-currents to the out-of-plane component σ_{zz}^I of nuclear shielding, were evaluated for $I = \mathrm{H}$ and C on the plane at 0.75 bohr, see Figures 2 and 3.

The shielding density maps for H1(α) and H5(β) protons of naphthalene in Figure 3 show different patterns. The π-current density $\mathbf{J^B}(\mathbf{r})$ at point $\mathbf{r}$ generates an element of magnetic field $d\mathbf{B}_{ind}(\mathbf{R}_H)$ that reinforces or diminishes $\mathbf{B}$ at the site of the proton, and produces magnetic deshielding or shielding on the probe, depending on the angle between the streamline at $\mathbf{r}$ and the distance vector $\mathbf{R}_H - \mathbf{r}$, i.e., on the sign of the vector product $\mathbf{J^B}(\mathbf{r}) \times (\mathbf{R}_H - \mathbf{r})$ in eq. (1).

Net overall deshielding effects from π-ring currents arise from molecular domains close to the proton under consideration. For both α and β hydrogens, a deshielding basin in the neighborhood of the adjacent carbon nucleus (C1 and C5, respectively) is observed as a dashed area of the contour maps. The minimum values of the shielding density function are almost the same, $\approx$22 au. On the other hand, the deshielding domain of H1(α) encompasses three conjugated carbon atoms in two rings, C1, C9, and C4, and major portions of the C1–C5 and C1–H1 bonds. It is much larger than that of H5(β), which contains only the C1–C5, C5–C7, and C5–H5 bonds.

Allowing for eqs. (1) and (5), the signature of π-ring currents is also evident in the weakly-shielding region of remote carbon atoms. Their positive contribution to σ_{zz}^H is comparatively negligible for both α and β protons. As emphasized above, these patterns depend on the angle θ between the vectors $\mathbf{J^B}(\mathbf{r})$ and $\mathbf{R}_H - \mathbf{r}$. Deshielding and shielding basins are separated by nodal contours in which $sin\theta$ vanishes, e.g., in the vicinity of the C4, C9, C5, and H1 atoms for α protons, and C1, C7, H5 for β protons in Figure 3.

By superimposing the contour shielding density and streamline maps with the same scale, reported in higher resolution as SMA, it is immediately verified that shielding (deshielding) regions correspond to negative (positive) values of $sin\theta$, see Fig. 10. Therefore, the different chemical shifts of α and β protons depends merely on geometrical factors, as the π-ring currents have nearly the same modulus in their proximity, see Appendix.

The small enhancement of $|\mathbf{J^B}(\mathbf{r})|$ intensity nearby the bridge carbons observed in the bottom right map of Figure 1 does not produce any major effect, c.f. the corresponding shielding density map in Figure 3. Moreover, the experimental downfield chemical shifts of α and β protons with respect to benzene, 0.41 and 0.06 ppm,[35] should be understood as mainly caused by higher intensity of π-ring currents in naphthalene. Stronger deshielding is actually predicted for the σ_{zz}^H components in $C_{10}H_8$, c.f. the theoretical π-contributions in Table 1 with the value -2.86 ppm in benzene,[12]

Table 2. Nuclear magnetic shieldings of symmetry unique atoms in the anthracene molecule (in ppm).[a]

Atom	Contr.	*xy*	*yx*	*xx*	*yy*	*zz*	*av*
C_1	σ+ core					156.03	
	π					13.13	
	Total	−29.90	−36.36	51.55	−51.58	169.16	56.38
	EXP[b]			44	−59	173	57.6
C_5	σ+ core					167.21	
	π					16.16	
	Total	−61.51	−57.84	−2.23	0.20	183.37	60.45
	EXP[b]			−28	12	183	60.4
C_9	σ+ core					175.46	
	π					26.91	
	Total	−15.22	−15.57	−22.98	−25.13	202.37	51.42
	EXP[b]			−41	−15	196	53.9
C_{13}	σ+ core					146.06	
	π					16.28	
	Total	0.00	0.00	54.42	−39.65	162.34	59.04
	EXP[b]			44	−48	161	59.5
H_1	σ+ core					22.90	
	π					−5.07	
	Total	−0.97	−0.94	29.35	23.96	17.83	23.71
	EXP[c]						22.91–23.02
H_5	σ+ core					23.13	
	π					−3.48	
	Total	−2.03	−1.42	27.07	26.67	19.65	24.46
	EXP[c]						23.44–23.56
H_{13}	σ+ core					22.58	
	π					−6.79	
	Total	0.00	0.00	30.18	23.45	15.79	23.14
	EXP[c]						22.48–22.59

[a] Via the CTOCD-DZ2 approach.
[b] See SMA for the procedure used to estimate experimental values.
[c] Quoted in Ref. 3.

and the small differences among contributions from σ-currents to σ_{zz}^H discussed above.

The strongly anisotropic shielding of carbon nuclei is determined by the interplay of several effects. For the three nonequivalent carbon atoms C1, C5, and C9, the average $\sigma_{\perp}^C$ in-plane components are negative, ≈ -2.5, ≈ -5.0, and ≈ -29.4 ppm, respectively. Their magnitude is much smaller than that of the big positive out-of-plane components σ_{zz}^C, 172.4, 185.3, and 202.1 ppm respectively, which increases in the opposite sense, see also SMA.

The current density and the shielding density maps show that these σ_{zz}^C values are mainly biased by intense diamagnetic σ-vortices localized in a small region around the carbon nucleus under consideration. Remarkably, the π-electron currents flowing close to the probe beyond the molecular perimeter, and about distant portions of the ring provide contributions to σ_{zz}^C as big as 10–15%, c.f. the estimates $\approx$15.8, $\approx$18.1, and $\approx$26.2 ppm, respectively, in Table 1, see also 3-dimensional maps in SMA.

A convincing explanation of these trends, which provide another typical hallmark of π-ring current effects on the out-of-plane component of the ^{13}C magnetic shielding,[14] is immediately arrived at via relationships (1)–(6), by superimposing the current density maps

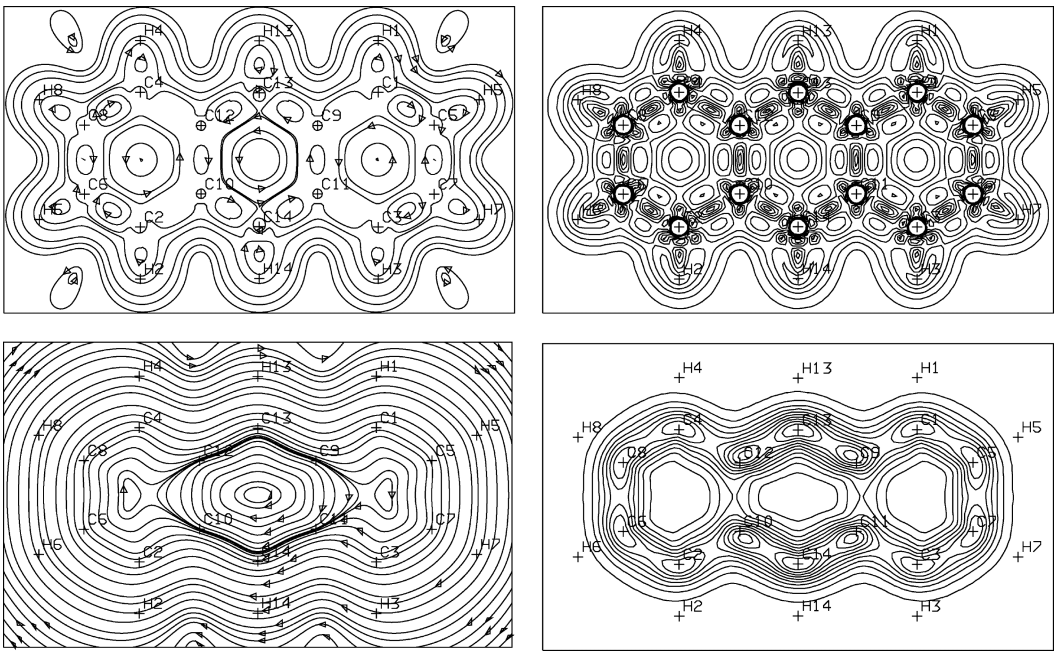

Figure 4. Streamlines and contour levels for the modulus of the total current density on the molecular plane of anthracene (above) and π-electron contributions on a plane at 0.75 bohr (below). Nuclear positions are marked with crosses. The applied magnetic field (of unit magnitude) points outward and diamagnetic flow is clockwise. The maximum modulus (contour step) values are 1.97 (cut to 0.2), and 0.11 (0.02 and 0.01), respectively, in au. The intense σ-electron flow spiralling in the proximity of C1-C9 bond and symmetry related loci is not represented.

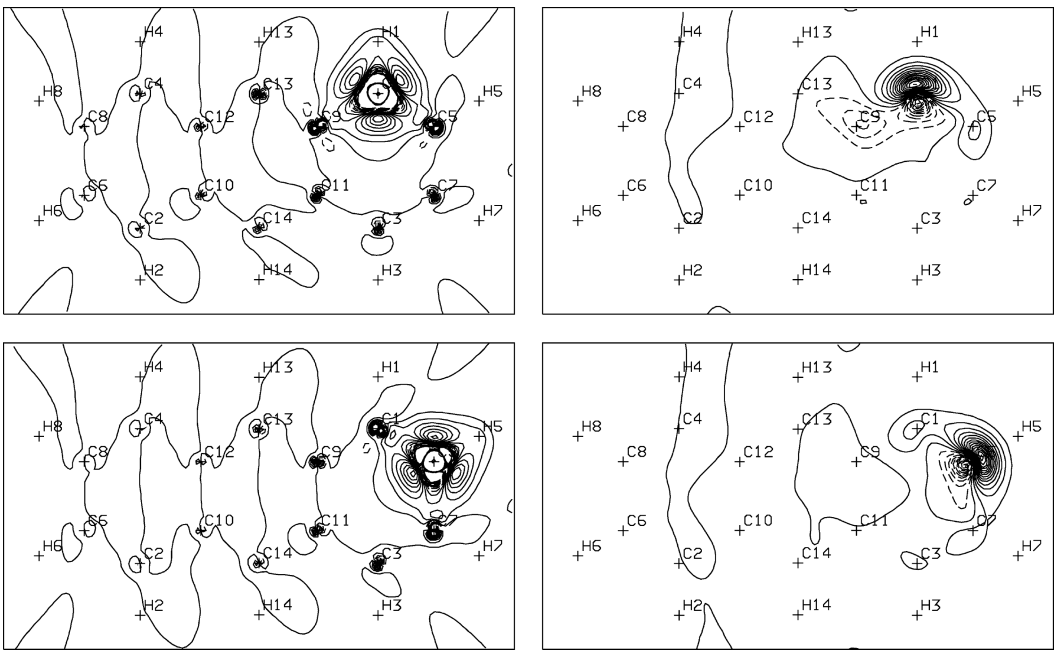

Figure 5. Magnetic shielding densities of carbon nuclei in anthracene, Σ_{zz}^{C1} (above) and Σ_{zz}^{C5} (below). σ-electron (π-electron) contributions on the molecular plane (on a plane at 0.75 bohr) are given on the left (right). In the contour map solid (dashed) lines mean positive (negative) values. Minimum (maximum) value of σ contributions are cut to -0.1 (0.1) and the contour step is 0.01. Minimum (maximum) values of π-contributions are -0.035 (0.042) and -0.034 (0.043) for C1 and C5 respectively. The contour step is 0.003.

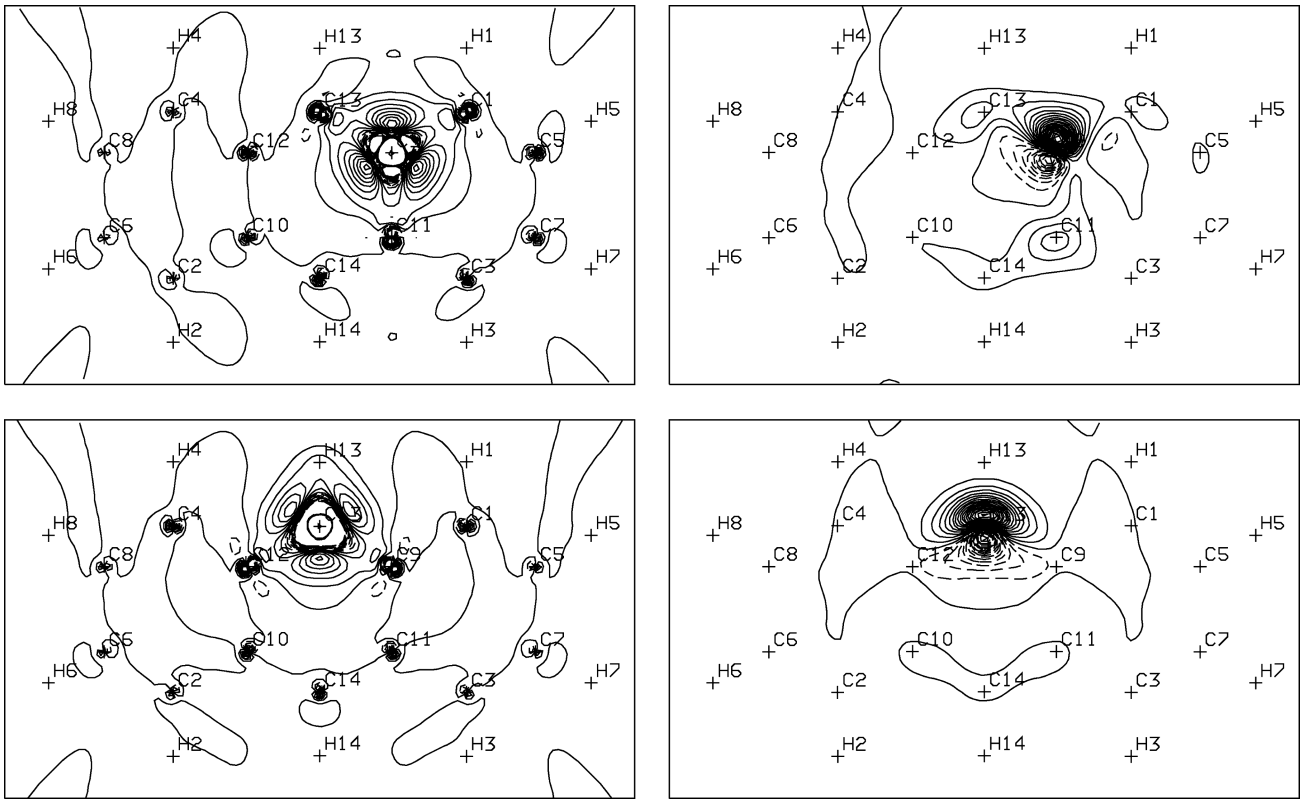

Figure 6. Magnetic shielding densities Σ_{zz}^{C9} (above) and Σ_{zz}^{C13} (below) of carbon nuclei in anthracene. σ-electron (π-electron) contributions on the molecular plane (on a plane at 0.75 bohr) are given on the left (right). In the contour map solid (dashed) lines mean positive (negative) values. Minimum (maximum) value of σ contributions are cut to -0.1 (0.1) and the contour step is 0.01. Minimum (maximum) values of π-contributions are -0.036 (0.063) and -0.054 (0.055) for C9 and C13 respectively. The contour step is 0.003.

in Figure 1 to the shielding densities in Figure 2 and observing the angle between $\mathbf{J^B}(\mathbf{r})$ and $\mathbf{R}_C - \mathbf{r}$.

Minor deshielding effects from the annular π-electron stream on σ_{zz}^{C1}, σ_{zz}^{C5}, and σ_{zz}^{C9} are confined to quite small basins inside the ring current circuit. Prevailing shielding contributions arise from much wider domains about the carbon framework. Other interesting features are worth observing, e.g., the nodal regions in the maps for C1 and C5, and the wide shielding basin all over the molecular perimeter in the map for most shielded σ_{zz}^{C9}. The different extension of the shielding domains explains the trend of values of π-electron contributions to σ_{zz}^{C1}, σ_{zz}^{C5}, and σ_{zz}^{C9}.

Theoretical magnetic shieldings of carbon and hydrogen nuclei in anthracene are reported in Table 2. The maps on bottom of Figure 4 show that the strength of the π circulation on a plane at 0.75 bohr from that of the molecule is greatest within the central ring. The maximum local modulus is 0.11 au, which can be compared with 0.09 in naphthalene. The higher intensity of the π currents determine stronger deshielding of anthracene protons in the same positions as naphthalene's. Trends similar to those observed for $C_{10}H_8$ are confirmed, see Figures 5–7: (i) the average in plane component $\sigma_\perp^C$ decreases in the same sequence as naphthalene's carbon nuclei similarly placed, calculated values in ppm being $\approx$7 for C_{13}, $\approx$0 for C_1, ≈ -1 for C_5, ≈ -24 for C_9; (ii) the $\sigma_\parallel^C$ out-of-plane component increases in the opposite sense, i.e., $\approx$162 for C_{13}, $\approx$169 for C_1, $\approx$183 for C_5, $\approx$202 for C_9, and it determines the strong anisotropy of the carbon shielding; (iii) the contribution of the π electron currents to $\sigma_\parallel^C$ is $\sim$10%, or a bit higher for C_9; (iv) the contribution of the σ electrons to $\sigma_\parallel^C$ is the same as naphthalene's to three significant figures; (v) the proton at C_{2v} symmetry site (H_{13} in the present study) is deshielded to higher extent owing to π ring currents that diminish the out-of-plane component $\sigma_\parallel^H$; (vi) the chemical shift between α and β protons is due to the same effects observed in naphthalene, $\sigma_\parallel^H$ of $H_1 \equiv \alpha$ being slightly more deshielded in anthracene.

Comparison with Experimental Data

The sequence of near Hartree-Fock CTOCD-DZ2 average shieldings in naphthalene, $\sigma_{av}^{C1} = 55.78$, $\sigma_{av}^{C5} = 58.42$, and $\sigma_{av}^{C9} = 47.77$ ppm, is consistent with experimental values[35] of carbon chemical shifts with respect to tetramethylsilane, $\delta^{C1} = 128.0$, $\delta^{C5} = 126.0$, and $\delta^{C9} = 133.7$ ppm. However, some discrepancies are observed, e.g., $\delta^{C9} - \delta^{C5} = 7.7$ ppm, whereas $\sigma_{av}^{C5} - \sigma_{av}^{C9} = 10.6$ ppm; $\delta^{C9} - \delta^{C1} = 5.7$, whereas $\sigma_{av}^{C1} - \sigma_{av}^{C9} \approx 8$ ppm. Preliminary calculations using correlated wavefunctions and smaller basis seem to

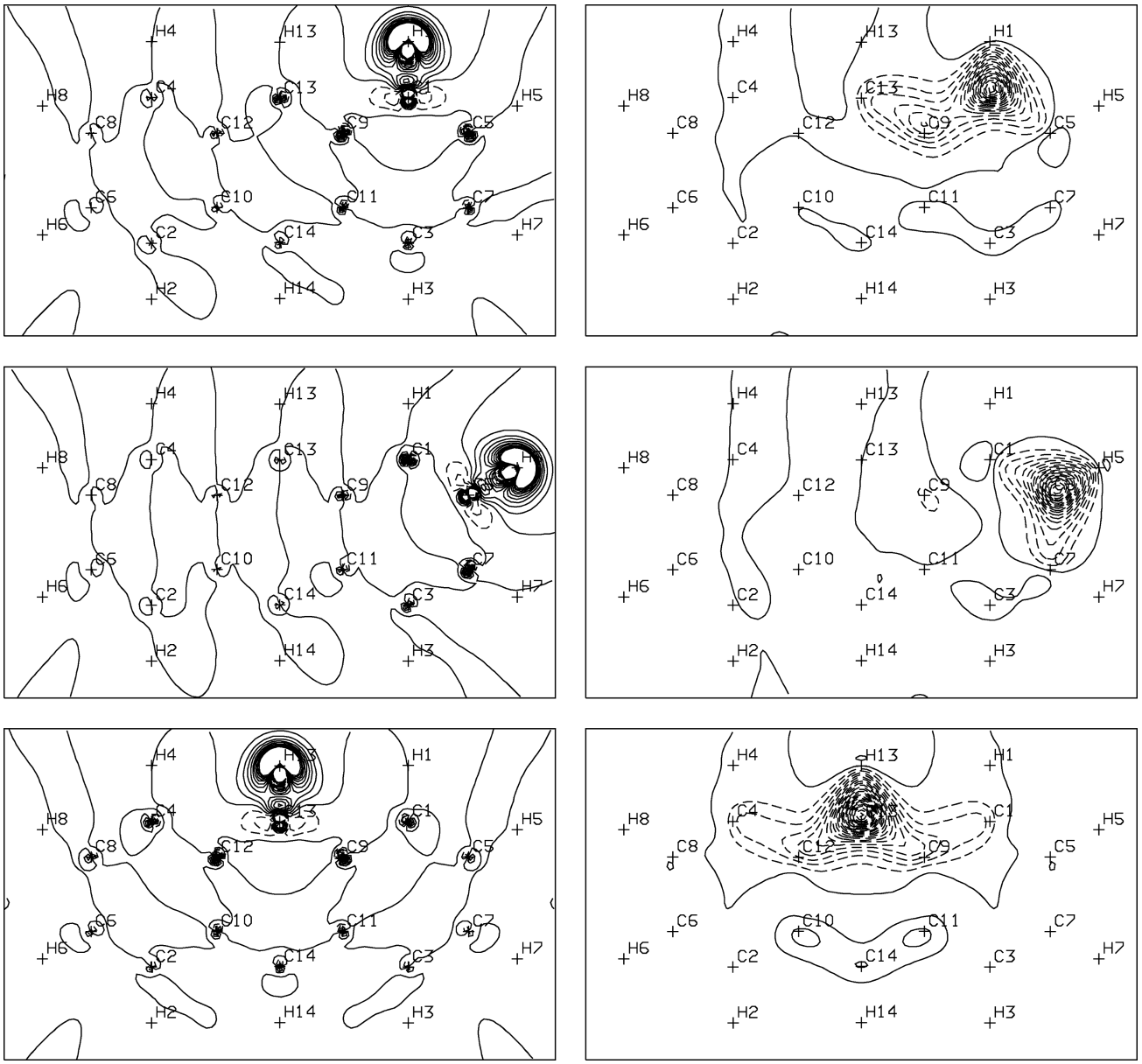

Figure 7. Magnetic shielding densities of protons in anthracene: from top to bottom Σ_{zz}^{H1}, Σ_{zz}^{H5} and Σ_{zz}^{H13}. σ-electron (π-electron) contributions on the molecular plane (on a plane at 0.75 bohr) are given on the left (right). Plotting conventions are the same as in Figure 2. Minimum (maximum) values of σ-electron contributions, in au, are cut to -0.1 (0.1 for all protons and the contour step is 0.01. Minimum (maximum) values of π-electron contributions, in au, are -0.018 (0.0018), -0.019 (0.0019) and -0.024 (0.0024) for H1, H5 and H13, respectively. The contour step is 0.001.

indicate that correlation effects are not very important in this context and, in fact, the discrepancies between $\Delta\delta$ and $\Delta\sigma$ are only diminished by $\approx$1 ppm.

Discrepancies with estimates of carbon shielding components from measurements in crystal and liquid crystal phase are larger. These may arise from the confusion caused by unclear conventions and notation, as well as referencing problems[41] of papers reporting experimental data for benzene,[37,43] naphthalene,[38,39] and anthracene,[44] see p. 63 of Ref. 36 and the SMA of the present paper. Therefore the procedures adopted here are fully described in the SMA section to help explain errors that have been possibly made via our assignments. A similar misunderstanding may affect also the estimates given in previous papers,[2,3] which are superseded by the present more accurate study. Another source of uncertainty arises from the definition of principal axes of the experimental chemical shift tensors.

A hermitian matrix has real eigenvalues and unitary eigenvectors. The shielding tensor $\sigma_{\alpha\beta}^{I}$ is not in general symmetric in the exchange

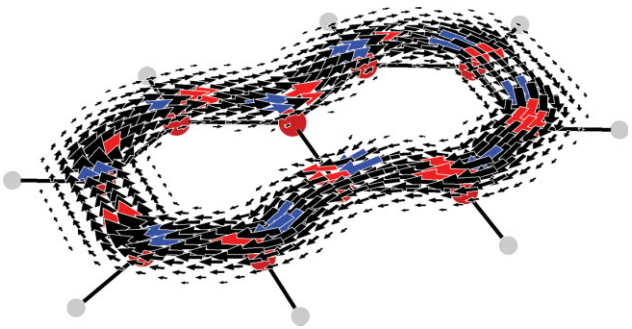

Figure 8. The π ring current density flowing around the perimeter of naphthalene in a magnetic field normal to the molecular plane. The size of the arrows is proportional to the local modulus $|\mathbf{J}^{\mathbf{B}}|$, which varies between 0.01 and 0.09 au. Red (blue) denote ascending (descending) currents. The 3-dimensional map can be rotated and magnified via the graphic code delivered by the authors.[†]

$\alpha \leftrightarrow \beta$, but it is diagonal in a Cartesian reference frame if the site symmetry is C_{2v} or higher,[45] as for C_9 of naphthalene, and C_{13} and H_{13} of anthracene. In the cases investigated here deviations from index symmetry are usually small, and the eigenvalues of $\sigma^C_{\alpha\beta}$ are real. However, the eigenvectors are not orthogonal, e.g., for C_1 and C_5 of naphthalene,

$$\begin{pmatrix} 0.1900 & 0.9708 & 0 \\ 0.9818 & -0.2399 & 0 \\ 0 & 0 & 1 \end{pmatrix}, \quad \begin{pmatrix} -0.7768 & 0.6462 & 0 \\ -0.6297 & -0.7632 & 0 \\ 0 & 0 & 1 \end{pmatrix}$$

with corresponding eigenvalues, in ppm, $\sigma^{C1}_{11} = -59.9$, $\sigma^{C1}_{22} = 54.9$, $\sigma^{C1}_{33} = 172.4$, $\sigma^{C5}_{11} = -62.3$, $\sigma^{C5}_{22} = 52.3$, $\sigma^{C5}_{33} = 185.3$. The eigenvector ϵ_3 is perpendicular to the plane of ϵ_1 and ϵ_2, which are not orthogonal to one another, and it is assumed to be at right angles to the molecular plane of naphthalene and anthracene, i.e., parallel to the z axis.

The estimates of experimental carbon shielding component reported in Tables 1 and 2 were obtained from chemical shift tensors.[37,38,43,44] Theoretical and experimental values of the out-of-plane component of carbon shielding seem to agree satisfactorily in most cases, much less so for the in-plane components. Discrimination between σ^C_{xx} and σ^C_{yy} is not obvious at all from the values of ref. 44 Actually in the cases where our results on anthracene differ the most from the experimental values, a significant improvement is achieved by simply swapping the 1 and 2 principal axes in ref. 44.

Therefore, our estimates of experimental σ^C_{xx} and σ^C_{yy} should be regarded with care. We hope however that the near Hartree-Fock results in this article may help future experimental assignments. It is desirable that new measurements were taken, or referenced, under conditions as close as possible to that of the isolated molecule assumed in the calculations, i.e., in the gas phase in the zero pressure limit.[41] Careful referencing is also needed for data from NMR in crystal and liquid crystal phase.[36]

Concluding Remarks

This article reports near Hartree-Fock estimates of magnetizability and magnetic shielding of hydrogen and carbon nuclei in the naphthalene and anthracene molecules. The excellent quality of the calculation was checked via closeness of theoretical results from a number of different approximated methods and by sum rules for gauge invariance and charge conservation, see the supplementary material available. Graphical information is given to complete the RCM of the naphthalene and anthracene systems by visualizing the effects of σ- and π-electron currents on the magnetic shielding of H and C nuclei via shielding density maps.[20,21]

In particular, the mechanism causing different chemical shifts of α and β protons in naphthalene has been investigated, providing a clear and reasonable solution to a long debated problem. The Biot-Savart law shows that the difference of ~0.35 ppm depends only on geometrical factors, as the π-ring current has nearly the same intensity all over the molecular perimeter. The effect should entirely be imputed to the out-of-plane component $\sigma^H_{\parallel}$ of the shielding tensor – the only one affected by π ring currents.

The α proton is more deshielded than β's because the domain in which the sine of the angle between the streamlines and the vector to the probe in α position has a negative value is much wider. All over this domain, which extends over three carbon nuclei for the former and only one for the latter, the induced Biot-Savart magnetic field reinforces the applied magnetic field, (see "Current density and shielding density maps" and "Response of arenes to a magnetic field normal to the molecular plane" Sections for details.

The strongly anisotropic shielding of ^{13}C nuclei can similarly be explained via current density and magnetic shielding density maps, documenting big contributions from an intense diamagnetic vortex about the carbon nuclei, induced by an external magnetic field normal to the molecular plane. This vortex causes strong

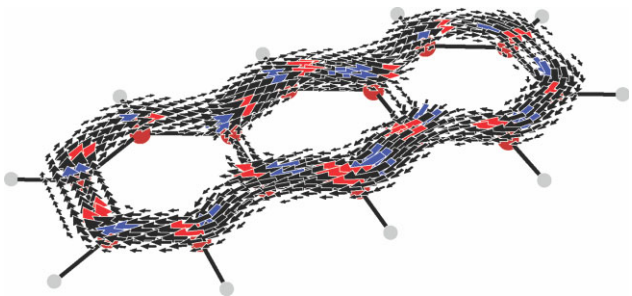

Figure 9. The π ring current density flowing around the perimeter of anthracene in a magnetic field normal to the molecular plane. The size of the arrows is proportional to the local modulus $|\mathbf{J}^{\mathbf{B}}|$, which varies between 0.01 and 0.11 au. Red (blue) denote ascending (descending) currents. The 3-dimensional map can be rotated and magnified via the graphic code delivered by the authors.

[†]The LINUX and WINDOWS versions of the graphic code used to obtain three-dimensional representations of the stagnation graph and current density vector field of a series of molecules can be downloaded at https://theochem.chimfar.unimo.it/VEDO3/naphthalene-anthracene.

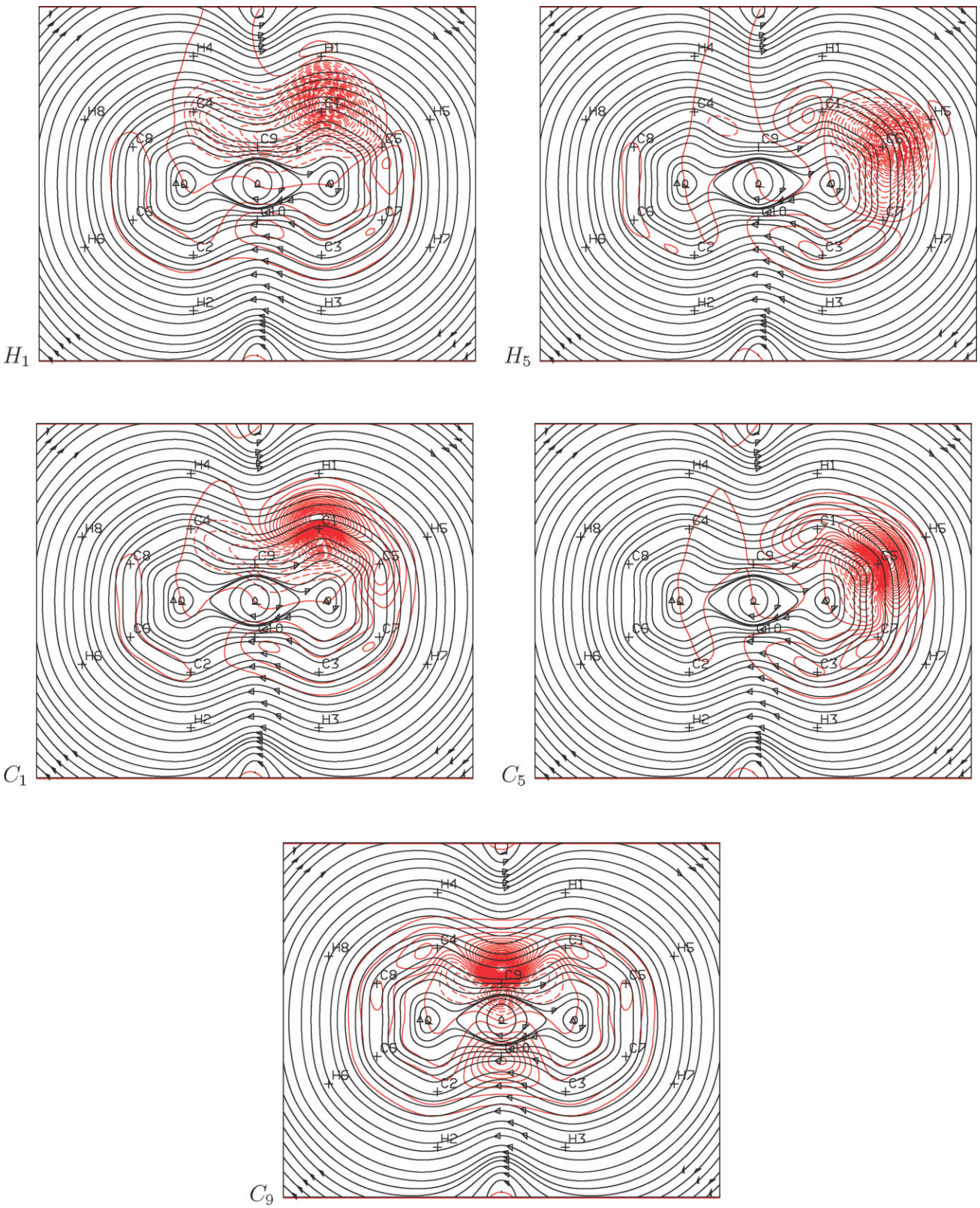

Figure 10. π-ring currents and corresponding shielding densities Σ_{zz}^{C} and Σ_{zz}^{H} in naphthalene.

enhancement of the positive out-of-plane component for the three non-equivalent carbon atoms of naphthalene. A positive contribution as big as 10–15% to the out-of-plane component of carbon shielding is also given by the π ring currents flowing beyond the C-skeleton, in front of the probe carbon, and in distant portions of the circuit.

The average in-plane components of the carbon shielding tensors are negative and they are much smaller – in absolute value, 7, 37, and 68 times, for the three different carbon nuclei – and, remarkably, increase in the opposite sense. The results obtained provide a general model, useful to rationalize NMR shifts of ^{1}H and ^{13}C also in related compounds, e.g., tetra-azanaphthalenes.[29] Such a model can arguably be extended to higher PAHs.

Similar conclusions are in fact arrived at by shielding density maps for anthracene. Three diamagnetic vortices sustained by the π electrons are observed in Figure 4 on the long axis of the molecule. The vortex flowing about the centre of the molecule is separated by two saddle points from those of the terminal rings. The resolution of the maps in this figure is much higher than in previous studies.[1,3] There is no trace of π paramagnetic vortices, supposed to appear in Figure 1 of ref. 3

Remarkably enough, the streamline and modulus maps in Figure 4 show that π ring currents are stronger all over the central ring of the anthracene molecule, on a plane 0.75 bohr above that of the molecule, where they reach a maximum value $|\mathbf{J}^{\mathbf{B}}| \approx 0.11$ au. Their intensity ($\approx$0.08) is nearly the same over the peripheral C–C bonds of the terminal rings, and it is comparable with naphthalene's. The π currents flow also along the internal C–C bonds, with intensity $\approx$0.04 au on the same plot plane. These values can be compared with the corresponding quantity for the π ring current in benzene, $\approx$0.08, on plane at similar distance.[10] A perspective view of the π current density showing the leap-frog effect[46] is reported in Figures 8 and 9.

The chemical shift between hydrogen nuclei at the peripheral sites with local C_s symmetry is rationalized as in naphthalene. The stronger deshielding of the central proton, at a locus with C_{2v} symmetry, is due to the low value of the out-of-plane component of the shielding tensor. Our calculations show that the deshielding arising from the π ring current is as big as ≈ -6.8 ppm, i.e., almost twice that of the α proton. The Biot-Savart law indicates that, also in this case, the deshielding region corresponds to a domain of points $\mathbf{r}$ in which the sine of the angle between $\mathbf{J}^{\mathbf{B}}(\mathbf{r})$ and $\mathbf{R}_H - \mathbf{r}$ is negative. The deshielding island is much wider for the central proton.

Acknowledgments

The authors like to thank Prof. J. C. Facelli for helpful discussions.

Appendix: Shielding densities superimposed to streamline maps

The induced Biot-Savart field is visualized, see Fig. 10, by superimposing the contour shielding density and corresponding streamline maps with the same scale, see Figures 1–3 for naphthalene. It can be verified that shielding (deshielding) regions correspond to negative (positive) values of $sin\theta$ as specified in the text. Magnified figures are reported as SMA also for anthracene.

References

1. Steiner, E.; Fowler, P. W. Int J Quantum Chem 1996, 60, 609.
2. Zanasi, R.; Lazzeretti, P. Mol Phys 1997, 92, 609.
3. Ligabue, A.; Pincelli, U.; Lazzeretti, P.; Zanasi, R. J Am Chem Soc 1999, 121, 5513.
4. Keith, T. A.; Bader, R. F. W. Chem Phys Lett 1993, 210, 223.
5. Lazzeretti, P.; Malagoli, M.; Zanasi, R. Chem Phys Lett 1994, 220, 299.
6. Zanasi, R. J Chem Phys 1996, 105, 1460.
7. von, Ragué Schleyer, P. Chem Rev 2001, 101, 1115.
8. von, Ragué Schleyer, P. Chem Rev 2005, 105, 3433.
9. Salem, L. The Molecular Orbital Theory of Conjugated Systems; W. A. Benjamin: New York, 1966.
10. Lazzeretti, P. In Progress in Nuclear Magnetic Resonance Spectroscopy, Vol 36; J. W. Emsley, J. Feeney, L. H. Sutcliffe, Eds.; Elsevier: Amsterdam, The Netherlands, 2000, pp. 1–88.
11. Lazzeretti, P.; Zanasi, R. Chem Phys Lett 1983, 100, 67.
12. Ferraro, M. B.; Lazzeretti, P.; Viglione, R. G.; Zanasi, R. Chem Phys Lett 2004, 390, 268.
13. Pelloni, S.; Ligabue, A.; Lazzeretti, P. Org Lett 2004, 6, 4451.
14. Ferraro, M. B.; Faglioni, F.; Ligabue, A.; Pelloni, S.; Lazzeretti, P. Magn Res Chem 2005, 43, 316.
15. Cuesta, I. G.; Jartín, R. S.; Sánchez de Merás, A.; Lazzeretti, P. J Chem Phys 2003, 119, 5518.
16. Cuesta, I. G.; Jartín, R. S.; Sánchez de Merás, A.; Lazzeretti, P. J Chem Phys 2004, 120, 6542.
17. Cuesta, I. G.; Jartín, R. S.; Sánchez de Merás, A.; Lazzeretti, P. Mol Phys 2005, 120, 789.
18. Cuesta, I. G.; Ligabue, A.; Sánchez de Merás, A.; Lazzeretti, P. Chem Phys Lett 2005, 401, 282.
19. Cuesta, I. G.; Sánchez de Merás, A.; Lazzeretti, P. J Comput Chem 2006, 27, 344.
20. Jameson, C. J.; Buckingham, A. D. J Phys Chem 1979, 83, 3366.
21. Jameson, C. J.; Buckingham, A. D. J Chem Phys 1980, 73, 5684.
22. Jackson, J. D. Classical Electrodynamics, John Wiley & Sons: New York, 3rd ed.; 1999, p. 178.
23. Heine, T.; Corminboeuf, C.; Seifert, G. Chem Rev 2005, 105, 3889.
24. Johnson, C. E.; Bovey, F. A. J Chem Phys 1958, 29, 1012.
25. Merino, G.; Heine, T.; Seifert, G. Chem Eur J 2004, 10, 4367.
26. Heine, T.; Islas, R.; Merino, G. J Comp Chem 2007, 105, 302.
27. Soncini, A.; Fowler, P. W.; Lazzeretti, P.; Zanasi, R. Chem Phys Lett 2005, 401, 164.
28. Fleischer, U.; Kutzelnigg, W.; Lazzeretti, P.; Mühlenkamp, V. J Am Chem Soc 1994, 116, 5298.
29. Cuesta, I. G.; Sánchez de Merás, A.; Lazzeretti, P. J Comput Chem 2006, 27, 1980.
30. Lazzeretti, P.; Malagoli, M.; Zanasi, R. Technical report on project "sistemi informatici e calcolo parallelo," Research Report 1/67, CNR, 1991.
31. Gaussian 03, Revision C.02, Frisch, M. J.; Trucks, G. W.; Schlegel, H. B.; Scuseria, G. E.; Robb, M. A.; Cheeseman, J. R.; Montgomery, Jr., J. A.; Vreven, T.; Kudin, K. N.; Burant, J. C.; Millam, J. M.; Iyengar, S. S.; Tomasi, J.; Barone, V.; Mennucci, B.; Cossi, M.; Scalmani, G.; Rega, N.; Petersson, G. A.; Nakatsuji, H.; Hada, M.; Ehara, M.; Toyota, K.; Fukuda, R.; Hasegawa, J.; Ishida, M.; Nakajima, T.; Honda, Y.; Kitao, O.; Nakai, H.; Klene, M.; Li, X.; Knox, J. E.; Hratchian, H. P.; Cross, J. B.; Bakken, V.; Adamo, C.; Jaramillo, J.; Gomperts, R.; Stratmann, R. E.; Yazyev, O.; Austin, A. J.; Cammi, R.; Pomelli, C.; Ochterski, J. W.; Ayala, P. Y.; Morokuma, K.; Voth, G. A.; Salvador, P.; Dannenberg, J. J.;

Zakrzewski, V. G.; Dapprich, S.; Daniels, A. D.; Strain, M. C.; Farkas, O.; Malick, D. K.; Rabuck, A. D.; Raghavachari, K.; Foresman, J. B.; Ortiz, J. V.; Cui, Q.; Baboul, A. G.; Clifford, S.; Cioslowski, J.; Stefanov, B. B.; Liu, G.; Liashenko, A.; Piskorz, P.; Komaromi, I.; Martin, R. L.; Fox, D. J.; Keith, T.; Al-Laham, M. A.; Peng, C. Y.; Nanayakkara, A.; Challacombe, M.; Gill, P. M. W.; Johnson, B.; Chen, W.; Wong, M. W.; Gonzalez, C.; and Pople, J. A.; Gaussian, Inc., Wallingford CT, 2004.

32. Lide, D. R. Ed. Handbook of Chemistry and Physics, 74th ed.; CRC Press: Boca Raton, 1993–1994.
33. Coriani, S.; Lazzeretti, P.; Malagoli, M.; Zanasi, R.; Theor Chim Acta 1994, 89, 181.
34. Zanasi, R.; Lazzeretti, P.; Malagoli, M.; Piccinini, F. J Chem Phys 1995, 102, 7150.
35. Pretsch, E.; Bühlmann, P. Affolter, C. Structure Determination of Organic Compounds: Tables of Spectral Data, 3rd ed., Springer Verlag: New York, 2000, p. 96, 180.
36. Jameson, C. J. In Specialist Periodical Reports-Nuclear Magnetic Resonance, Vol. 27, S. R. G. A. Webb, The Royal Society of Chemistry: Cambridge, 1998, pp. 44–82.
37. Strub, H.; Beeler, A. J.; Grant, D. M.; Michl, J.; Cutts, P. W.; Zilm, K. W. J Am Chem Soc 1983, 105, 3333.
38. Sherwood, M. H.; Facelli, J. C.; Alderman, D. W.; Grant, D. M. J Am Chem Soc 1991, 113, 750.
39. Facelli, J. C.; Grant, D. M. Nature 1993, 365, 325.
40. Grant, D. M.; Liu, F.; Iuliucci, R. J.; Phung, C. G.; Facelli, J. C.; Alderman, D. W. Acta Cryst B 1995, 51, 540.
41. Jameson, A. K.; Jameson, C. J. Chem Phys Lett 1987, 134, 461.
42. Breitmaier, E.; Haas, G.; Voelter, W. Atlas of Carbon-13 NMR Data; Heyden: London, 1979.
43. Linder, M.; Höner, A.; Ernst, R. J Mag Res 1979, 35, 379.
44. Tarroni, R.; Zannoni, C. J Phys Chem 1996, 100, 17157.
45. Raynes, W. T.; Ratcliffe, R. Mol Phys 1976, 37, 571.
46. Ligabue, A.; Soncini, A.; Lazzeretti, P. J Am Chem Soc 2002, 124, 2008.